

University of Nebraska - Lincoln  
**DigitalCommons@University of Nebraska - Lincoln**

---

Xiao Cheng Zeng Publications

Published Research - Department of Chemistry

---

2019

# Reaction mechanism between small-sized Ce clusters and water molecules: An ab initio investigation on $Ce_n+H_2O$

Rulong Zhou

*Hefei University of Technology*, [rlzhou@hfut.edu.cn](mailto:rlzhou@hfut.edu.cn)

Yang Yang

*Hefei University of Technology*

Seema Pande

*University of Nebraska - Lincoln*, [seema.pande@huskers.unl.edu](mailto:seema.pande@huskers.unl.edu)

Bingyan Qu

*Hefei University of Technology*

Dongdong Li

*Hefei University of Technology*

*See next page for additional authors*

Follow this and additional works at: <https://digitalcommons.unl.edu/chemzeng>

Part of the [Analytical Chemistry Commons](#), [Materials Chemistry Commons](#), and the [Physical Chemistry Commons](#)

---

Zhou, Rulong; Yang, Yang; Pande, Seema; Qu, Bingyan; Li, Dongdong; and Zeng, Xiao Cheng, "Reaction mechanism between small-sized Ce clusters and water molecules: An ab initio investigation on  $Ce_n+H_2O$ " (2019). *Xiao Cheng Zeng Publications*. 160.

<https://digitalcommons.unl.edu/chemzeng/160>

This Article is brought to you for free and open access by the Published Research - Department of Chemistry at DigitalCommons@University of Nebraska - Lincoln. It has been accepted for inclusion in Xiao Cheng Zeng Publications by an authorized administrator of DigitalCommons@University of Nebraska - Lincoln.

---

**Authors**

Rulong Zhou, Yang Yang, Seema Pande, Bingyan Qu, Dongdong Li, and Xiao Cheng Zeng

# Reaction mechanism between small-sized Ce clusters and water molecules: An *ab initio* investigation on $Ce_n + H_2O$

Rulong Zhou,<sup>1</sup> Yang Yang,<sup>1</sup> Seema Pande,<sup>2</sup> Bingyan Qu,<sup>1</sup>  
Dongdong Li,<sup>1</sup> and Xiao Cheng Zeng<sup>2</sup>

<sup>1</sup> School of Materials Science and Engineering, Hefei University of Technology,  
Hefei, Anhui 230009, P. R. China

<sup>2</sup> Department of Chemistry and Nebraska Center for Materials and Nanoscience,  
University of Nebraska-Lincoln, Lincoln, Nebraska 68588, USA

*Email:* rlzhou@hfut.edu.cn ; xzeng1@unl.edu

## Abstract

Reactions of small-sized cerium clusters  $Ce_n$  ( $n = 1-3$ ) with a single water molecule are systematically investigated theoretically. The ground state structures of the  $Ce_n/H_2O$  complex and the reaction pathways between  $Ce_n + H_2O$  are predicted. Our results show the size-dependent reactivity of small-sized Ce clusters. The calculated reaction energies and reaction barriers indicate that the reactivity between  $Ce_n$  and water becomes higher with increasing cluster size. The predicted reaction pathways show that the single Ce atom and the  $Ce_2$  and  $Ce_3$  clusters can all easily react with  $H_2O$  and dissociate the water molecule. Under UV-irradiation, the reaction of a Ce atom with a single  $H_2O$  molecule may even release an  $H_2$  molecule. The reaction of either  $Ce_2$  or  $Ce_3$  with a single  $H_2O$  molecule can fully dissociate the  $H_2O$  into H and O atoms while it is bonded with the Ce cluster. The electronic configuration and oxidation states of the Ce atoms in the products and the higher occupied molecular orbitals are analyzed by using the natural bond orbital (NBO) analysis method, from which the high reactivity between the reaction products of  $Ce_n + H_2O$  and an additional  $H_2O$  molecule is predicted. Our results offer deeper molecular insights into the chemical reactivity of Ce, which could be helpful for developing more efficient Ce-doped or Ce-based catalysts.

---

Published in *Physical Chemistry Chemical Physics* 21 (2019), pp 4006–4014.

DOI: 10.1039/c8cp07551d

Copyright © the Owner Societies; published by Royal Society of Chemistry. Used by permission.

Submitted 11 December 2018; accepted 21 January 2019.

Supplementary information is presented following the References.

## Introduction

Ce exhibits an intriguing electronic configuration of  $4f^15d^16s^2$  with the energy level of the inner-shell 4f orbital being very close to those of the valence orbitals. As such, the localized 4f electron of Ce can become itinerant and contribute to chemical bonding in certain cases. The easy transition of the 4f electron between localized and itinerant states means that the valence states of Ce are easily changeable so that Ce can adopt multivalence states such as +3 and +4 as well as mixed or intermediate valence states in different compounds. The transition from the localized state to the itinerant state of the 4f electron is also involved in the fascinating properties of Ce-based bulk materials, *e.g.* pressure-induced first-order phase transition with either Ce crystal<sup>1</sup> or liquid,<sup>2</sup> or with some Ce-based metallic glasses.<sup>3</sup> Due to the changeability between the  $Ce^{3+}$  and  $Ce^{4+}$  oxidation states, cerium oxide (ceria) exhibits excellent catalytic properties and has been widely used as a stand-alone or supporting material for many catalytic reactions, such as the water–gas shift reaction,<sup>4</sup> steam reforming of organics,<sup>5</sup> and reduction and oxidation reactions,<sup>6</sup> among others. An improved knowledge of the specific features of different oxidation states of Ce and the transition between them at the atomic and molecular levels is of importance for understanding the reactivity and catalytic properties of the cerium oxide surface. Towards this end, cerium oxide clusters and their reactions with small gaseous molecules have been extensively investigated both experimentally and theoretically.<sup>7–12</sup>

Recently, the reactions between a single Ce atom and various small gaseous molecules have been extensively investigated by means of the matrix-isolation infrared spectroscopy technique and high-level quantum chemistry calculations.<sup>13–18</sup> Li *et al.* studied the reaction of a single Ce atom with methanol molecules. They found that the Ce atom can react with two methanol molecules to form  $H_2$  and a Ce(II) complex of  $Ce(OCH_3)_2$  under annealing, and the Ce(II) complex can transform into a more stable Ce(IV) complex under UV-visible irradiation.<sup>13</sup> Xu *et al.* found that a single Ce atom can react with silane, forming a hydrogen bridged complex of  $Si(m-H)_3CeH$  (Ce is in the Ce(II) oxidation state) under annealing, which is different from the reaction between the Ce atom and  $CH_4$ , from which only the insertion  $H_3CCeH$  structure can be formed.<sup>14</sup> The experiments performed for studying the reaction between the Ce atom and  $H_2O_2$  molecules showed that

the Ce atoms are in the +2 and +3 oxidation states in the major products and in the +4 oxidation states in the minor products.<sup>15,16</sup>

Among all the reactions, the reaction between Ce and water molecules is of particular importance due to the relevance of producing H<sub>2</sub> fuel from water. Although the reactions between other lanthanides and H<sub>2</sub>O have been extensively investigated in experiments, experimental studies on the reaction between Ce with H<sub>2</sub>O are still scarce. Mikulas *et al.* studied the reaction between lanthanides and a single H<sub>2</sub>O molecule by using density functional theory with the B3LYP functional. They proposed that HCeOH and CeO + H<sub>2</sub> are possible main reaction products of the reaction.<sup>18</sup> However, the pathways for the reaction between Ce and a H<sub>2</sub>O molecule to form HCeOH or CeO + H<sub>2</sub> were not studied in that work, and the associated major product is still unclear. Moreover, the Ce atom may react with more H<sub>2</sub>O molecules to form high-oxidation-state cerium hydroxides, and the associated reaction pathways have not been studied thus far.

Besides the Ce atom, small Ce clusters may also possess high reactivity, and the reactivity of the Ce cluster can be strongly dependent on the cluster size and geometry. The oxidation states of the Ce atoms in the reaction products of the Ce clusters and gaseous molecules will also be very different from those of a single Ce atom. Hence, a systematic study of the reaction between small Ce clusters and gaseous molecules will be helpful to achieve deeper understanding of the reactive properties of Ce and to develop high-performance Ce-based catalysts.

In this work, we systematically studied the reactions between a single Ce atom and H<sub>2</sub>O molecules, as well as between a small Ce cluster (Ce<sub>2</sub> or Ce<sub>3</sub>) and H<sub>2</sub>O molecules, based on combined global structural search and density functional theory (DFT) calculations. Possible reaction products of the reactions involving Ce, Ce<sub>2</sub> and Ce<sub>3</sub> with different numbers of H<sub>2</sub>O molecules are predicted. The reaction pathways of Ce<sub>*n*</sub> + H<sub>2</sub>O and Ce<sub>*n*</sub> + 2H<sub>2</sub>O towards the energetically most stable products are computed. The associated electronic configuration and oxidation states of Ce atoms in all the products are analyzed. Here, we will only report the results of the reactions of Ce<sub>*n*</sub> + H<sub>2</sub>O. Those of the reactions between Ce<sub>*n*</sub> and more than one H<sub>2</sub>O molecule will be reported in our forthcoming paper. Our results show that a single Ce atom may react with one H<sub>2</sub>O molecule to release an H<sub>2</sub> molecule under UV irradiation, while Ce<sub>2</sub> and Ce<sub>3</sub> can fully dissociate the H<sub>2</sub>O molecule. The reactivity of Ce<sub>*n*</sub> with H<sub>2</sub>O shows a size-dependent feature.

## Computational method

The ground-state structures of the product from the reaction between the Ce atom or Ce clusters and H<sub>2</sub>O were obtained from the combined structural search and DFT calculations. The low-lying candidate isomers of the reaction products were obtained from the structural search using the evolutionary algorithm implemented in the Universal Structure Predictor: Evolutionary Xtallography (USPEX) package.<sup>19,20</sup> 150 structures were generated randomly in the first generation with the constraint of various point group symmetries. 30 isomers were generated in the subsequent generations by performing various evolutionary operations. The structural relaxation of each isomer was performed using the plane-wave density functional theory (DFT) method implemented in the VASP 5.4 package.<sup>21,22</sup> The Perdew–Burke–Erzerhof (PBE) exchange–correlation functional<sup>23</sup> and an energy cutoff of 400 eV are adopted in the structural optimization using the VASP package. The projector augmented wave (PAW) pseudopotentials are chosen to describe the interactions of elements, for which the number of valence electrons of H, O, and Ce are 1, 6 and 11, respectively. The isomers with distinct geometrical structures and low energies (within 0.1 eV per atom from the lowest-energy isomer) were identified for the next-stage high-level structural optimization.

The low-lying isomers selected from the structural search were re-optimized at a higher level of DFT using the hybrid B3LYP functional, implemented in the Gaussian 09 program.<sup>24,25,26</sup> All-electron 6-311++G(d,p) basis sets were used for H and O atoms. For the Ce atoms, the energy-consistent effective-core potential (ECP) with 28 core electrons and the SDD basis set were adopted.<sup>27,28</sup> The geometries were fully relaxed *via* an analytic gradient algorithm, followed by vibrational frequency calculation to ensure that each geometry was optimized into a local minimum. We also performed two other benchmark computations at the CAM-B3LYP/6-311++G(d,p) (SDD for Ce) and dispersion-corrected B3LYP/TZP(ZORA) levels of theory, respectively. Both levels of theory give very close results to the B3LYP/6-311++G(d,p) (SDD for Ce) level of theory used in this work.

The reaction pathways between the Ce clusters and the H<sub>2</sub>O molecules were explored using a two-step approach. Firstly, we employed the nudged-elastic-band (NEB) method implemented in the VTST code<sup>29–32</sup> combined with the VASP package to search for possible

low-barrier reaction pathways. Since there could be several intermediate states in the reaction pathway, a sole NEB search is not enough to explore all the possible intermediate states and transition states. Hence, several NEB searches are performed. Specifically, from the first-step NEB search, we can obtain a rough minimum-energy path (MEP) between the reactant and product. There may be several local minima on the MEP curve, which may correspond to the intermediate states. Based on the local minima on the MEP curve, we split the reaction path into several segments, and for each segment, a second-step NEB search is performed. For a particular segment, if there were also local minima existing on the MEP curve from the second NEB search, further splitting of the reaction route and a third-step NEB search would be performed. Lastly, for each segment, there is only one saddle point in the MEP curve, which corresponds to the transition state of this segment. In each NEB search, ten images are inserted between the original and final images.

Secondly, the structure at each saddle point in the MEP curve is selected as the initial guess for the transition-state structure and then optimized using the Broyden algorithm implemented in Gaussian 09 to obtain the optimized transition state structure.<sup>33</sup> Next, the intrinsic reaction coordinates (IRC) analysis is performed in both the forward and backward directions to obtain the reactant and product geometries of this segment.

## Results and discussion

### **1. The reaction path between Ce<sub>n</sub> and a single H<sub>2</sub>O molecule**

**(a) Reaction: Ce + H<sub>2</sub>O.** We first study the reaction between a Ce atom and a single water molecule. The structural search and DFT calculation at the B3LYP/6-311++G(d,p) (SDD for Ce) level of theory reveal that the ground-state structure of the product is CeO + H<sub>2</sub> as shown in **Figure 1(e)**, a mixture of CeO and H<sub>2</sub> molecules. This result shows that a single Ce atom may be capable of decomposing a water molecule into hydrogen under certain conditions.

The Ce + H<sub>2</sub>O reaction starts from Ce(H<sub>2</sub>O) (Fig. 1(a)), *i.e.* molecular adsorption of H<sub>2</sub>O on the Ce atom. The reactant is 2.491 eV higher in total energy than the product. Based on the computed reaction

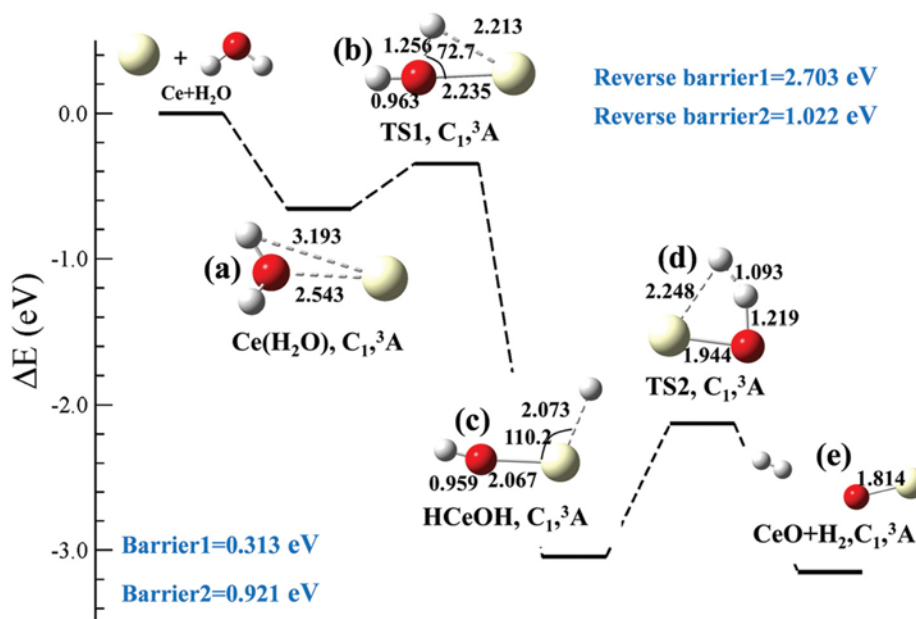


**Fig. 1.** The energy diagram and the structures of the reactant (a), intermediate (c), transition states (b) and (d), and product (e), involved in the Ce + H<sub>2</sub>O reaction. The energies are calculated at the B3LYP/6-311++G(d,p) (SDD for the Ce atoms) level.

path, there exists an intermediate state HCeOH (Fig. 1(c)), whose energy is 0.101 eV higher than that of the product. In HCeOH, the H<sub>2</sub>O molecule is dissociatively adsorbed on the Ce atom. The length of the Ce–O bond is 2.067 Å, about 0.2 Å shorter and longer than the length of the Ce–O bond in the reactant Ce(H<sub>2</sub>O) and product CeO + H<sub>2</sub>, respectively. The structures of the first transition state from the reactant Ce(H<sub>2</sub>O) to the intermediate HCeOH, and the second from the intermediate to the product CeO + H<sub>2</sub>, denoted as TS1 and TS2, are shown in Fig. 1(b) and (d), respectively.

The energy diagram for the reaction between a Ce atom and a single H<sub>2</sub>O molecule is shown in Fig. 1. The energy barrier of the first-step reaction is 0.313 eV and that of the reverse reaction is 2.703 eV. The much lower barrier for the forward reaction compared to that of the backward reaction means that the forward reaction is dominant under ambient conditions. The energy barrier of the second-step reaction is 0.921 eV, suggesting that this reaction can occur under ambient conditions along with certain stimulations, *e.g.* UV-visible irradiation. The barrier of the reverse second-step reaction is 1.022 eV, very close



to that of the forward reaction. Hence, the possibilities from HCeOH to CeO + H<sub>2</sub> and from CeO + H<sub>2</sub> to HCeOH are very close. Overall, for the reaction between a Ce atom and a single H<sub>2</sub>O molecule, the major reaction product is expected to be HCeOH at room temperature, whereas under irradiation, CeO + H<sub>2</sub> can be major products as well.

**(b) Reaction: Ce<sub>2</sub> + H<sub>2</sub>O.** For the reaction between a Ce<sub>2</sub> cluster and a single H<sub>2</sub>O molecule, the ground state structure is H<sub>2</sub>Ce<sub>2</sub>O, as shown in **Figure 2**(g), with the H<sub>2</sub>O molecule being fully dissociated, and the H and O atoms being bonded with both Ce atoms. H<sub>2</sub>Ce<sub>2</sub>O has C<sub>2v</sub> symmetry. The H<sub>2</sub>O can also adsorb on the Ce<sub>2</sub> cluster through the Ce–O bond, forming Ce<sub>2</sub>(H<sub>2</sub>O) (see Fig. 2(a)). It is 4.180 eV higher in energy than the ground-state structure H<sub>2</sub>Ce<sub>2</sub>O. Starting from Ce<sub>2</sub>(H<sub>2</sub>O), the reaction undergoes two intermediate states prior to the formation of H<sub>2</sub>Ce<sub>2</sub>O. The first intermediate state is named CeHCeOH (Fig. 2(c)). The structure at the first transition state, from Ce<sub>2</sub>(H<sub>2</sub>O) to CeHCeOH, is named TS1 (Fig. 2(b)). The adsorbed H<sub>2</sub>O molecule in Ce<sub>2</sub>(H<sub>2</sub>O) rotates

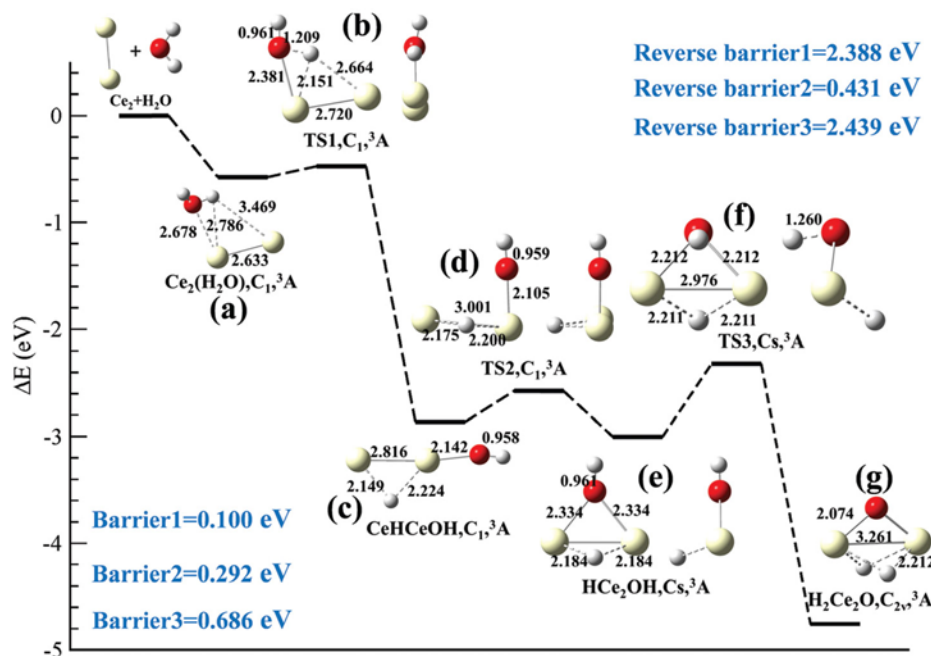


**Fig. 2.** The energy diagram and the structures of the reactant (a), intermediates (c) and (e), transition states (b), (d) and (f), and product (g) involved in the Ce<sub>2</sub> + H<sub>2</sub>O reaction. The energies are calculated at the B3LYP/6-311++G(d,p) (SDD for the Ce atoms) level.

towards the other Ce atom. The interaction between one of the H atoms and the two Ce atoms becomes stronger as they are closer. Eventually, the H–O bond is broken due to the strong interaction between Ce and the H atom, forming CeHCeOH. The hydroxyl group in CeHCeOH can also easily rotate around the bonded Ce atom. When it rotates near the Ce–Ce bond center, another Ce–O bond is formed, giving the second intermediate HCe<sub>2</sub>OH (Fig. 2(e)). The transition state from CeHCeOH to HCe<sub>2</sub>OH is named TS2 (see Fig. 2(d)). The reaction from HCe<sub>2</sub>OH to H<sub>2</sub>Ce<sub>2</sub>O needs to pass the transition state TS3 (Fig. 2(f)). The H atom of the hydroxyl group in HCe<sub>2</sub>OH rotates around the O atom, and when it is close enough to the Ce atoms, two Ce–H bonds are formed, leading to the ground-state structure H<sub>2</sub>Ce<sub>2</sub>O.

The energy diagram of the reaction between Ce<sub>2</sub> and H<sub>2</sub>O is also shown in Fig. 2. The energy barrier of each reaction step is 0.100 eV, 0.298 eV and 0.686 eV, respectively. The corresponding reverse energy barriers are 2.388 eV, 0.431 eV and 2.439 eV, respectively. According to the energy barriers, the first-step and second-step reactions proceed more easily than the third step at room temperature. So the abundance of the intermediate HCe<sub>2</sub>OH is likely higher than that of the ground state structure.

**(c) Reaction: Ce<sub>3</sub> + H<sub>2</sub>O.** The reaction between a Ce<sub>3</sub> cluster and a single H<sub>2</sub>O molecule is much more complicated than those associated with Ce and Ce<sub>2</sub>. Our structural search shows that there are several low-lying structures with close energies. The ground-state structure is H<sub>2</sub>Ce<sub>3</sub>O, as shown in **Figure 3(k)**, with the H<sub>2</sub>O molecule being fully dissociated and each atom bonded with two Ce atoms of the Ce<sub>3</sub> cluster. For other close-energy structures, the positions of H atoms are different. Moreover, H<sub>2</sub>O can also molecularly adsorb on the Ce<sub>3</sub> cluster (named Ce<sub>3</sub>(H<sub>2</sub>O), as shown in Fig. 3(a)). The latter is much higher in energy (5.539 eV) than the ground-state structure H<sub>2</sub>Ce<sub>3</sub>O. Ce<sub>3</sub>(H<sub>2</sub>O) can transform into H<sub>2</sub>Ce<sub>3</sub>O through five-step reactions, passing through four intermediate states (named INT1–INT4, as shown in Fig. 3(c, e, g and i)) and five transition states (named TS1–TS5, as shown in Fig. 3(b, d, h and j)). The relative energies of the intermediates INT1 to INT4 with respect to the ground state structure are 2.817 eV, 2.269 eV, 2.183 eV, and 0.205 eV, respectively. The full reaction path can be depicted as follows: firstly, the adsorbed H<sub>2</sub>O molecule rotates around the bonded Ce atom towards the center of the

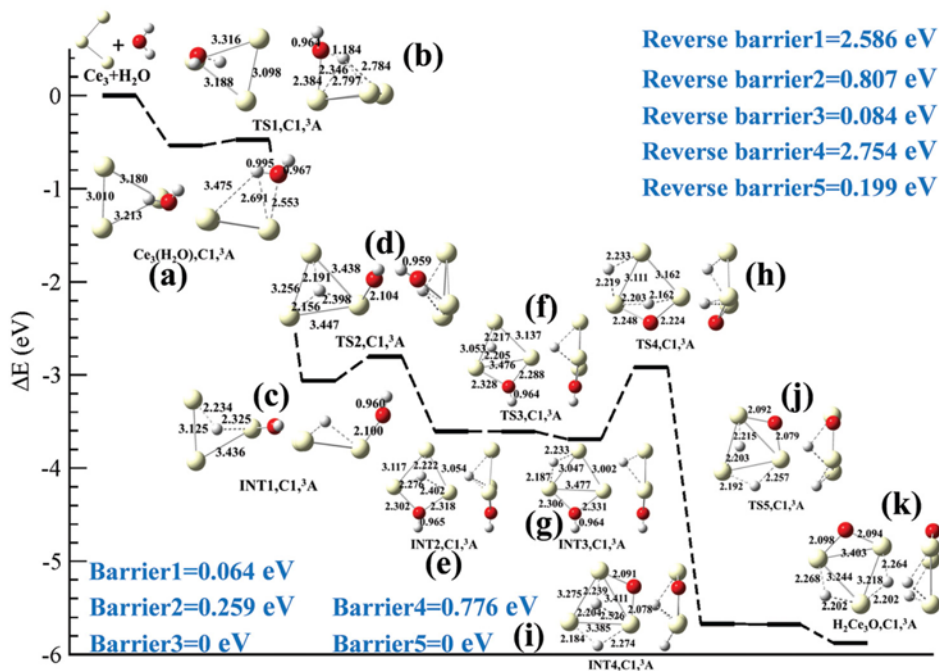


**Fig. 3.** The energy diagram and the structures of the reactant (a), intermediate states (c), (e), (g), and (i), transition states (b), (d), (f), (h), and (j) and product (g) involved in the  $\text{Ce}_3 + \text{H}_2\text{O}$  reaction. The energies are calculated at the B3LYP/6-311++G(d,p) (SDD for the Ce atoms) level.

$\text{Ce}_3$  trimer. Then, one O–H bond of  $\text{H}_2\text{O}$  is broken due to the interaction between an H atom and Ce atoms, forming INT1. Secondly, the hydroxyl group rotates around the bonded Ce atom (named Ce1) towards one of the other Ce atoms (named Ce2). Then, INT1 transforms into INT2. Thirdly, the dissociated H atom from  $\text{H}_2\text{O}$  moves from the center to the outside of the  $\text{Ce}_3$  triangle, and the structure transforms into INT3. Fourthly, the hydroxyl group rotates around the bonded side towards the center of the  $\text{Ce}_3$  triangle, and then the other H is dissociated from the hydroxyl group. The structure transforms from INT3 into INT4. The last step is similar to the third step, where the H atom in the center moves to the outside of the  $\text{Ce}_3$  triangle.

The energy diagram of the reaction between a  $\text{Ce}_3$  cluster and a single  $\text{H}_2\text{O}$  molecule is shown in Fig. 3. The energy barrier from the reactant  $\text{Ce}_3(\text{H}_2\text{O})$  to INT1 is 0.064 eV, whereas the barrier of the reverse reaction is 3.134 eV. Hence,  $\text{Ce}_3(\text{H}_2\text{O})$  is dynamically unstable and can easily transform into INT1. For the second-step reaction, the energy barriers of the forward and reverse reactions are 0.259 eV and

0.807 eV, respectively. The notable difference between the two barriers means that the reaction from INT1 to INT2 is easy and nearly irreversible. The transition between INT2 and INT3 will be very easy because the energy barriers of both the forward and reverse reactions between INT2 and INT3 are very low, being 0 eV and 0.084 eV, respectively. The energy barrier from INT3 to INT4 is 0.776 eV, which can be overcome by high-energy excitation. Once INT4 is formed, it can easily transform into the ground state structure because the energy barrier is almost zero, from INT4 to  $\text{H}_2\text{Ce}_3\text{O}$ . Based on the energy diagram, we expect that the intermediate structures INT2 and INT3 may have relatively high abundance in the reaction product, while under high-energy excitation (e.g. UV-visible irradiation), INT4 and  $\text{H}_2\text{Ce}_3\text{O}$  can also form.

## 2. Reactivities of $\text{Ce}_n$ with a single $\text{H}_2\text{O}$ molecule

In order to evaluate the reactivity of  $\text{Ce}_n$  with a single water molecule, we calculated the reaction energy of each reaction, as listed in **Table 1**. Apparently, for all the Ce clusters concerned, the reaction with a water molecule to the ground state product is exothermic. The exothermic energies increase with the increase in the cluster size, meaning that a larger Ce cluster may more easily react with a  $\text{H}_2\text{O}$  molecule to form more stable products.

The critical steps of each reaction are the dissociation of the first and second H atom. The energy barrier of the first H's dissociation can reflect the reactivity of the  $\text{Ce}_n$  cluster, and that of the second H's

**Table 1.** Reaction energies of the reactions of  $\text{Ce}_n + \text{H}_2\text{O}$ , binding energy of  $\text{Ce}_n(\text{H}_2\text{O})$ , and the barrier energies of the dissociation of the 1st and 2nd H in each reaction.

Reaction	Reaction energy (eV)	Energy barrier (eV)		
		Dissociation of 1st H	Dissociation of 2nd H	Adsorption energy (eV)
$\text{Ce} + \text{H}_2\text{O} \rightarrow \text{CeO} + \text{H}_2$	-3.149	0.313	0.921	0.657
$\text{Ce}_2 + \text{H}_2\text{O} \rightarrow \text{H}_2\text{Ce}_2\text{O}$	-4.757	0.100	0.686	0.576
$\text{Ce}_3 + \text{H}_2\text{O} \rightarrow \text{H}_2\text{Ce}_3\text{O}$	-5.876	0.064	0.766	0.536

dissociation reflects the difficulty in yielding the ground state product. The calculated energy barriers of the first and second H's dissociations are also listed in Table 1. For the dissociation of the first H, the energy barrier in the reaction of  $\text{Ce} + \text{H}_2\text{O}$  is 0.313 eV, while those in the reactions of  $\text{Ce}_2 + \text{H}_2\text{O}$  and  $\text{Ce}_3 + \text{H}_2\text{O}$  are not higher than 0.1 eV, meaning that the reactions between  $\text{Ce}_2$  or  $\text{Ce}_3$  and a single  $\text{H}_2\text{O}$  molecule are much easier than that between a Ce atom. Moreover, as the cluster size increases, the energy barrier of the first H dissociation decreases monotonically, indicating that the reactivity of  $\text{Ce}_n$  with  $\text{H}_2\text{O}$  increases with the increase of the cluster size, at least in the size range of  $n \leq 3$ .

For the dissociation of the second H, the energy barriers are all much higher than those of the 1st H. The energy barrier of the second H's dissociation in the reaction of  $\text{Ce} + \text{H}_2\text{O}$  is also obviously larger than those of the reactions of  $\text{Ce}_2 + \text{H}_2\text{O}$  and  $\text{Ce}_3 + \text{H}_2\text{O}$ , similar to that of the 1st H's dissociation. However, the energy barriers of the second H's dissociation do not decrease monotonically with the increase in the cluster size. The lower energy barrier of the dissociation of the second H atom also indicates that the reactivities of  $\text{Ce}_2$  and  $\text{Ce}_3$  are higher than that of the single Ce atom.

In order to understand the size-dependent reactivity of  $\text{Ce}_n$  with  $\text{H}_2\text{O}$ , we first consider the binding between the  $\text{H}_2\text{O}$  molecule and  $\text{Ce}_n$ . As listed in Table 1, the adsorption energy of  $\text{H}_2\text{O}$  on  $\text{Ce}_n$  decreases slightly with the increase in cluster size, indicating that the binding of a single Ce atom with  $\text{H}_2\text{O}$  is a little stronger compared to those of  $\text{Ce}_2$  and  $\text{Ce}_3$  with  $\text{H}_2\text{O}$ . All the values are very small. Usually, a higher adsorption energy means a higher reactivity, so the size dependent reactivity of  $\text{Ce}_n$  with  $\text{H}_2\text{O}$  has little relation with the binding between  $\text{Ce}_n$  and the  $\text{H}_2\text{O}$  molecule.

As discussed in the above subsection, the dissociation of H from the adsorbed  $\text{H}_2\text{O}$  needs the assistance of the neighboring Ce atoms. So the Ce–H interaction plays an important role in the dissociation of H from the adsorbed  $\text{H}_2\text{O}$ . The Ce–H distance can characterize the overlap of the outmost atomic orbitals of H and Ce atoms and reflect the interaction between Ce and H atoms. As seen in Fig. 1–3, the distance between H1 (the first dissociated H atom) and Ce1 (directly bonded with  $\text{H}_2\text{O}$ ) in the reactant is 3.193 Å in  $\text{Ce}(\text{H}_2\text{O})$ , 2.786 Å in  $\text{Ce}_2(\text{H}_2\text{O})$ , and 2.691 Å in  $\text{Ce}_3(\text{H}_2\text{O})$ . So, the Ce1–H1 interaction in  $\text{Ce}(\text{H}_2\text{O})$  is much weaker than those in  $\text{Ce}_2(\text{H}_2\text{O})$  and  $\text{Ce}_3(\text{H}_2\text{O})$  due

to the much longer Ce1–H1 distance. Hence, owing to the difference in the Ce1–H1 interaction, it should be easier for the adsorbed H<sub>2</sub>O in Ce<sub>2</sub>(H<sub>2</sub>O) and Ce<sub>3</sub>(H<sub>2</sub>O) to tilt towards the Ce1 atom, compared to Ce(H<sub>2</sub>O). Moreover, as the H<sub>2</sub>O tilts towards Ce1, the interaction between H1 and the other Ce atoms in Ce<sub>2</sub>(H<sub>2</sub>O) and Ce<sub>3</sub>(H<sub>2</sub>O) becomes stronger, which further helps in moving H1 towards the Ce clusters. In Ce(H<sub>2</sub>O), because only one Ce atom exists, the movement of H1 towards the Ce atom is surely more difficult compared to that in Ce<sub>2</sub>(H<sub>2</sub>O) and Ce<sub>3</sub>(H<sub>2</sub>O). Hence, the barrier of the dissociation of the first H in the reaction of Ce + H<sub>2</sub>O is much higher than that in the reaction of Ce<sub>2</sub> + H<sub>2</sub>O and Ce<sub>3</sub> + H<sub>2</sub>O.

For the dissociation of the second H atom, as seen in Fig. 1–3, the distances between H2 and the nearest Ce atoms in HCeOH of the Ce + H<sub>2</sub>O reaction, HCe<sub>2</sub>OH of the Ce<sub>2</sub> + H<sub>2</sub>O reaction, and INT3 of the Ce<sub>3</sub> + H<sub>2</sub>O reaction are all longer than 3.0 Å. Moreover, the OH radical and the Ce atom in HCeOH are almost in the same line, and the OH radical and the Ce<sub>*n*</sub> clusters in HCe<sub>2</sub>OH and INT3 are almost in the same plane. So the outermost atomic orbitals of H2 and the Ce atoms cannot overlap directly. As such, the interaction between H2 and the Ce atoms in these intermediate structures is much weaker, compared to the interaction between H1 and the Ce atoms in the reactants. Hence, the dissociation of the second H in each reaction is much more difficult than that of the first H.

### **3. Electronic structures of the reaction products**

The products of the reaction between Ce<sub>*n*</sub> and a single H<sub>2</sub>O molecule may further react with additional H<sub>2</sub>O or other gas molecules. The reactivity is correlated with the valence states of the Ce atoms and the frontier molecular orbitals. We first computed the electronic properties of the stable structure of the reaction products of Ce<sub>*n*</sub> + H<sub>2</sub>O using the Natural Bond Orbital (NBO) analysis method. The charges of Ce, O and H atoms, and the electronic configuration of Ce atoms in various products are listed in **Table 2**. Based on the data, the valence states of the Ce atoms in each structure are determined, as listed in Table 2.

For the reaction of Ce + H<sub>2</sub>O, there may be two stable reaction products (CeO and HCeOH). The Ce atom adopts the Ce(II) oxidation state in both structures. Because Ce can mostly adopt the Ce(IV)

**Table 2.** Natural bond orbital (NBO) analysis for the main products of the  $\text{Ce}_n + \text{H}_2\text{O}$  ( $n = 1-3$ ) reactions.

Reaction	Isomers	Charge			Valence state (Ce)	Population of Ce
		Ce	O	H		
$\text{Ce} + \text{H}_2\text{O}$	HCeOH	1.24	-1.19	-0.54	+2	$4f^{1.12}5d^{0.78}6s^{0.82}$
	CeO	1.07	-1.07	0.50	+2	$4f^{1.22}5d^{0.77}6s^{0.92}$
$\text{Ce}_2 + \text{H}_2\text{O}$	HCe <sub>2</sub> OH	0.58	-1.20	-0.46	+1	$4f^{1.16}5d^{1.47}6s^{0.74}$
		0.58	0.49		+1	$4f^{1.16}5d^{1.47}6s^{0.74}$
	H <sub>2</sub> Ce <sub>2</sub> O	1.04	-1.20	-0.44	+2	$4f^{1.15}5d^{0.95}6s^{0.78}$
		1.04	-0.44		+2	$4f^{1.12}5d^{0.91}6s^{0.83}$
$\text{Ce}_3 + \text{H}_2\text{O}$	INT3	0.41	-1.18	-0.42	+0.5	$4f^{1.13}5d^{1.47}6s^{0.65}$
		0.71	0.49		+1.5	$4f^{1.12}5d^{1.48}6s^{0.96}$
		0.00			0	$4f^{1.12}5d^{2.09}6s^{0.77}$
	H <sub>2</sub> Ce <sub>3</sub> O	0.92	-1.20	-0.45	+1.5	$4f^{1.13}5d^{1.31}6s^{0.60}$
		0.90	-0.44		+1.5	$4f^{1.13}5d^{1.35}6s^{0.54}$
		0.27			+1.0	$4f^{1.08}5d^{1.93}6s^{0.66}$

oxidation state, CeO and HCeOH can further react with additional H<sub>2</sub>O molecules. In the CeO structure, as seen in Table 2, Ce transfers about 1.07e to O, forming a covalent Ce–O bond. In the HCeOH structure, Ce is bonded with an H atom and a hydroxyl radical, donating 0.5e and 0.74e to H1 and the OH radical, respectively. The O atom in CeO and HCeOH accepts 1.07e and 1.19e, respectively. So when the intermediate structure HCeOH transforms into the ground state product CeO + H<sub>2</sub>, some electrons transfer back from the O atoms to the Ce atom, which mainly occupy the 4f and 6s orbitals of Ce.

For the reaction of  $\text{Ce}_2 + \text{H}_2\text{O}$ , in the lowest-energy product H<sub>2</sub>Ce<sub>2</sub>O, each of the H and O atoms is bonded with both Ce atoms. As shown in Table 2, both H atoms and the O atom draw electrons from the Ce atoms, forming Ce–H and Ce–O bonds. So each Ce atom is in the Ce(II) oxidation state. In the intermediate state structure HCe<sub>2</sub>OH, both Ce atoms adopt the Ce(I) oxidation state because they contribute electrons equally to the H1 atom and the OH radical. Both structures can also react with additional H<sub>2</sub>O molecules because the Ce atoms in them do not reach their maximum oxidation states.

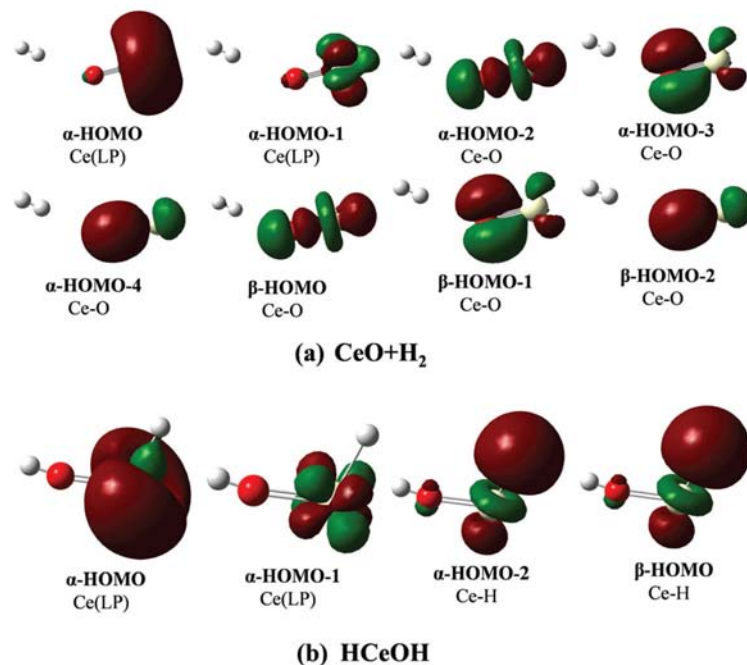
The valence states of the Ce atoms in the reaction products of  $\text{Ce}_3 + \text{H}_2\text{O}$  are very complicated. In  $\text{H}_2\text{Ce}_3\text{O}$  (the lowest-energy product of  $\text{Ce}_3 + \text{H}_2\text{O}$  reaction), both H atoms draw electrons from the Ce atoms, and they are both in  $-1$  valence states. The O atom is in the  $-2$  valence state as usual. As a consequence, the overall  $\text{Ce}_3$  cluster should be in the  $+4$  valence state. For different Ce atoms, the two Ce atoms (Ce1 and Ce2) bonded with O should possess valence states between  $+1$  and  $+2$  because they not only share the O atom with each other but also share one H atom with the third Ce atom (Ce3). Ce3 shares the two H atoms with Ce1 and Ce2, respectively, and it should be in the  $+1$  state. Hence, considering the symmetry, the valence states of Ce1 and Ce2 should be  $+1.5$ . In another possible reaction product of  $\text{Ce}_3 + \text{H}_2\text{O}$ , the intermediate state INT3, the  $\text{H}_2\text{O}$  molecule dissociatively adsorbs on the  $\text{Ce}_3$  cluster, as shown in Fig. 3. So the  $\text{Ce}_3$  cluster should be in the valence state of  $+2$ . For individual atoms, as listed in Table 2, Ce1 to Ce3 possess positive charges of 0.41, 0.71 and 0.0, respectively. The H atom bonded with Ce1 and Ce2 draws 0.42e from the Ce atoms, and the other H atom donates 0.49e to the O atom. So 0.69e are transferred from Ce1 and Ce2 to O. From the charges of all the atoms in INT3, we can suppose that the valence states of Ce1 to Ce3 are  $+0.5$ ,  $+1.5$  and 0, respectively.

From the oxidation states of the Ce atoms in the intermediate and ground state products of each reaction, we can speculate that the intermediate product should be more reactive than the ground state product because the oxidation states of the Ce atoms in the intermediate products are usually lower than those in the ground state products. Moreover, the reactivity of the products of  $\text{Ce}_n + \text{H}_2\text{O}$  should increase with the increase in the cluster size  $n$ . The results of the reaction between  $\text{Ce}_n$  with additional  $\text{H}_2\text{O}$  molecules will be reported in our forthcoming paper.

To further evaluate the reactivity of the reaction products of  $\text{Ce}_n + \text{H}_2\text{O}$ , the frontier molecular orbitals of the stable products are also studied. Because the dissociation of H from the  $\text{H}_2\text{O}$  molecule needs electron transfer from the cerium hydroxide during the reaction, we only consider the occupied frontier molecular orbitals.

Several higher occupied molecular orbitals of the reaction products of  $\text{Ce} + \text{H}_2\text{O}$  are shown in **Figure 4**, and the corresponding eigenvalues and the compositions of these are listed in the supplementary information, **Table S1**. For both CeO and HCeOH, the topmost

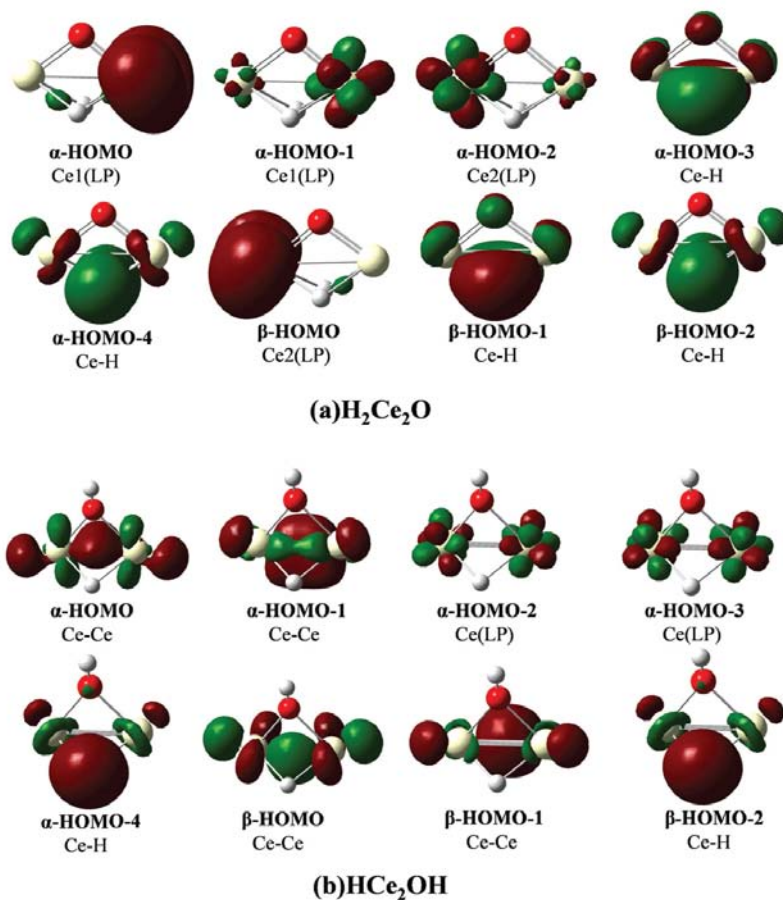




**Fig. 4.** The high-energy occupied molecular orbitals of the reaction products of  $\text{Ce} + \text{H}_2\text{O}$ .

two occupied molecular orbitals for alpha spin come from the Ce atom, and the other higher occupied molecular orbitals correspond to the Ce–O or Ce–H bonds. For each structure, the HOMO is a hybridization of the valence atomic orbitals of Ce, mostly composed of the 6s orbital, while the HOMO–1 is the localized 4f atomic orbital of Ce. Since the electrons on HOMO and HOMO–1 all come from the Ce atom, they can easily transfer to the gas molecules during the reaction. So CeO and HCeOH surely can react with another  $\text{H}_2\text{O}$  or other gas molecules.

For the reaction products of  $\text{Ce}_2 + \text{H}_2\text{O}$ , as shown in **Figure 5**, there are eight occupied molecular orbitals composed of Ce-based orbitals for both the ground state structure  $\text{H}_2\text{Ce}_2\text{O}$  and the intermediate structure HCe<sub>2</sub>OH. For  $\text{H}_2\text{Ce}_2\text{O}$ , the topmost three occupied MOs of the alpha spin and the HOMO of the beta spin all come from the Ce lone-pair (LP) orbitals. The Ce–H bond MOs correspond to relatively lower energies. The HOMO of the alpha spin is due to the hybridization of the Ce 6s and 5d orbitals, and the other Ce LP orbitals are all originated from the localized 4f orbital of Ce. Totally, four electrons

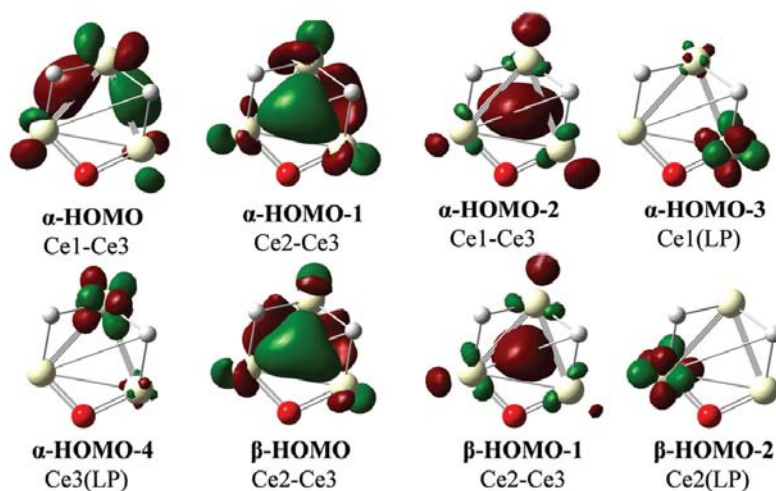
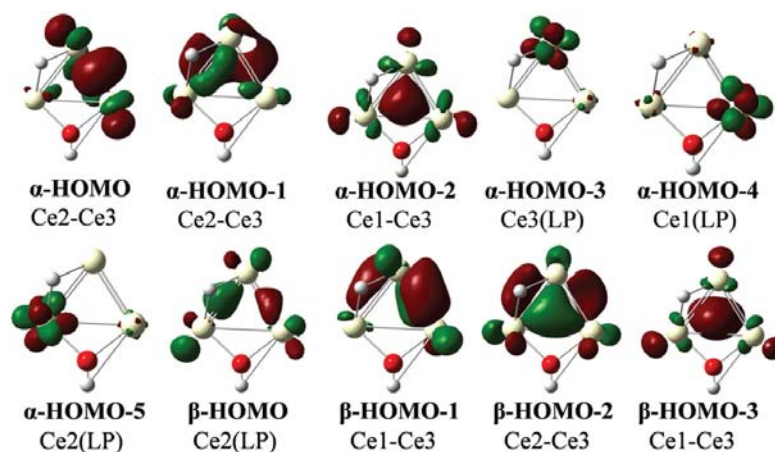


**Fig. 5.** Higher occupied molecular orbitals of the reaction products of  $\text{Ce}_2 + \text{H}_2\text{O}$ .

occupy the Ce LP orbitals, and both Ce atoms are in the Ce(II) oxidation states. The electrons occupying the Ce LP orbitals will assist the reaction of  $\text{H}_2\text{Ce}_2\text{O}$  with additional  $\text{H}_2\text{O}$  or other gas molecules.

For  $\text{HCe}_2\text{OH}$ , the topmost two occupied MOs of both alpha and beta spins correspond to the Ce–Ce bonds, which are mainly composed of the 6s and 5d orbitals of Ce. The HOMO–2 and HOMO–3 of the alpha spin of  $\text{HCe}_2\text{OH}$  are LP orbitals of Ce, which correspond to the localized 4f atomic orbitals of Ce1 and Ce2, respectively. There are totally six electrons occupying the MOs of the Ce–Ce bonds or the Ce LP orbitals, so in  $\text{HCe}_2\text{OH}$ , both Ce atoms are in Ce(I) oxidation states. More  $\text{H}_2\text{O}$  may react with  $\text{HCe}_2\text{OH}$  due to the abundant valence electrons on the Ce atoms.

The higher occupied molecular orbitals of the products  $\text{H}_2\text{Ce}_3\text{O}$  and INT3 of the  $\text{Ce}_3 + \text{H}_2\text{O}$  reaction are shown in **Figure 6**. The topmost

(a)  $\text{H}_2\text{Ce}_3\text{O}$ 

(b) INT3

**Fig. 6.** Higher occupied molecular orbitals of the reaction products of  $\text{Ce}_3 + \text{H}_2\text{O}$ .

eight MOs of  $\text{H}_2\text{Ce}_3\text{O}$  and the topmost ten MOs of INT3 all come from the Ce atoms. For both structures, the five higher occupied MOs correspond to the Ce–Ce bonds, and the other MOs correspond to the LP orbitals of Ce. Ce3 contributes to all the MOs of the Ce–Ce bonds, so there are more electrons on Ce3 compared to Ce1 and Ce2. The electrons can easily transfer among the Ce atoms. The high number of electrons on the Ce atoms ensures that both  $\text{H}_2\text{Ce}_3\text{O}$  and INT3 possess high reactivity with additional  $\text{H}_2\text{O}$  molecules.

## Conclusion

In conclusion, the chemical reactions between a single Ce atom, Ce<sub>2</sub> or Ce<sub>3</sub> clusters and a single water molecule are investigated theoretically by using combined global structural search and DFT calculations, as well as the reaction paths search method. The reaction pathways of Ce<sub>n</sub> + H<sub>2</sub>O are predicted. Based on the predicted ground state structures of the reaction products of Ce<sub>n</sub> + H<sub>2</sub>O, the reaction energies are calculated. The calculated reaction energies and the barriers of the reactions indicate that the reactivity of a Ce cluster with water increases as the size increases. The size-dependent reactivity is explained based on the overlapping of the Ce and H orbitals. Our studies show that a single Ce atom can easily react with a water molecule to form the HCeOH molecule under ambient conditions, while under UV-irradiation, an H<sub>2</sub> molecule can be released. Ce<sub>2</sub> and Ce<sub>3</sub> can more easily dissociate a water molecule into the H and OH radical, forming an HCe<sub>n</sub>OH complex. Both clusters can fully dissociate the water molecule into isolated atoms under UV-irradiation. The electronic structures of the possible reaction products are analyzed, with which the oxidation states of Ce are evaluated. Moreover, based on the electronic structure analysis, we predict that all products possess high reactivity and can react with additional water molecules.

**Conflicts of interest** — The authors have no conflicts to declare.

**Acknowledgments** — This work is supported by the NSAF Joint Funds of the National Natural Science Foundation of China (Grant No. U1630118). The numerical calculations have been done using the supercomputing systems at the Supercomputing Center of the University of Science and Technology of China and at the UNL Holland Computing Center.

## References

- 1 K. A. Gschneidner, L. Eyring and G. H. Lander, *Handbook on the physics and chemistry of rare earths*, Elsevier, 2002.
- 2 A. Cadien, Q. Y. Hu, Y. Meng, Y. Q. Cheng, M. W. Chen, J. F. Shu, H. K. Mao and H. W. Sheng, *Phys. Rev. Lett.*, 2013, 110, 125503.
- 3 H. W. Sheng, H. Z. Liu, Y. Q. Cheng, J. Wen, P. L. Lee, W. K. Luo, S. D. Shastri and E. Ma, *Nat. Mater.*, 2007, 6, 192–197.

- 4 Q. Fu, H. Saltsburg and M. Flytzani-Stephanopoulos, *Science*, 2003, 301, 935–938.
- 5 H. Takamura, T. Kobayashi, T. Kasahara, A. Kamegawa and M. Okada, *J. Alloys Compd.*, 2006, 408, 1084–1089.
- 6 A. Martinez-Arias, M. Fernández-García, J. Soria and J. Conesa, *J. Catal.*, 1999, 182, 367–377.
- 7 T. Nagata, K. Miyajima, R. A. Hardy, G. F. Metha and F. Mafune, *J. Phys. Chem. A*, 2015, 119, 5545–5552.
- 8 J. A. Felton, M. Ray, S. E. Waller, J. O. Kafader and C. C. Jarrold, *J. Phys. Chem. A*, 2014, 118, 9960–9969.
- 9 S. Hirabayashi and M. Ichihashi, *Chem. Phys. Lett.*, 2013, 564, 16–20.
- 10 S. Hirabayashi and M. Ichihashi, *J. Phys. Chem. A*, 2013, 117, 9005–9010.
- 11 X. N. Wu, X. L. Ding, S. M. Bai, B. Xu, S. G. He and Q. Shi, *J. Phys. Chem. C*, 2011, 115, 13329–13337.
- 12 F. Aubriet, J. J. Gaumet, W. A. de Jong, G. S. Groenewold, A. K. Gianotto, M. E. McIlwain, M. J. Van Stipdonk and C. M. Leavitt, *J. Phys. Chem. A*, 2009, 113, 6239–6252.
- 13 Y. Z. Li, Y. Gong, X. J. Zhou, J. Su, J. Li and M. F. Zhou, *J. Mol. Spectrosc.*, 2015, 310, 50–56.
- 14 B. Xu, P. Shi, T. Huang and X. Wang, *J. Mol. Struct.*, 2017, 1146, 692–702.
- 15 X. Wang, L. Andrews, Z. Fang, K. S. Thanthiriwatte, M. Chen and D. A. Dixon, *J. Phys. Chem. A*, 2017, 121, 1779–1796.
- 16 Z. Fang, K. S. Thanthiriwatte, D. A. Dixon, L. Andrews and X. Wang, *Inorg. Chem.*, 2016, 55, 1702–1714.
- 17 Z. Pu, W. Yu, S. K. Roy, C. Li, B. Ao, T. Liu, M. Shuai and X. Wang, *Phys. Chem. Chem. Phys.*, 2017, 19, 8216–8222.
- 18 T. C. Mikulas, M. Chen, Z. Fang, K. A. Peterson, L. Andrews and D. A. Dixon, *J. Phys. Chem. A*, 2016, 120, 793–804.
- 19 C. W. Glass, A. R. Oganov and N. Hansen, *Comput. Phys. Commun.*, 2006, 175, 713–720.
- 20 A. O. Lyakhov, A. R. Oganov, H. T. Stokes and Q. Zhu, *Comput. Phys. Commun.*, 2013, 184, 1172–1182.
- 21 G. Kresse and J. Furthmüller, *Phys. Rev. B: Condens. Matter Mater. Phys.*, 1996, 54, 11169.
- 22 G. Kresse and J. Hafner, *Phys. Rev. B: Condens. Matter Mater. Phys.*, 1993, 47, 558.
- 23 J. P. Perdew, K. Burke and M. Ernzerhof, *Phys. Rev. Lett.*, 1996, 77, 3865.
- 24 M. Frisch, G. Trucks, H. Schlegel, G. Scuseria, M. Robb, J. Cheeseman, G. Scalmani, V. Barone, B. Mennucci and G. Petersson, *Gaussian 09, revision b.01*, Gaussian, Inc., Wallingford, CT, 2010, 6492.
- 25 A. D. Becke, *J. Chem. Phys.*, 1993, 98, 5648–5652.

- 26 C. Lee, W. Yang and R. G. Parr, *Phys. Rev. B: Condens. Matter Mater. Phys.*, 1988, 37, 785.
- 27 M. Dolg, H. Stoll and H. Preuss, *J. Chem. Phys.*, 1989, 90, 1730–1734.
- 28 X. Cao and M. Dolg, *J. Mol. Struct. THEOCHEM*, 2002, 581, 139–147.
- 29 D. Sheppard and G. Henkelman, *J. Comput. Chem.*, 2011, 32, 1769–1771.
- 30 D. Sheppard, R. Terrell and G. Henkelman, *J. Chem. Phys.*, 2008, 128, 134106.
- 31 G. Henkelman, B. P. Uberuaga and H. Jónsson, *J. Chem. Phys.*, 2000, 113, 9901–9904.
- 32 G. Henkelman and H. Jónsson, *J. Chem. Phys.*, 2000, 113, 9978–9985.
- 33 C. Gonzalez and H. B. Schlegel, *J. Chem. Phys.*, 1989, 90, 2154–2161.

## Electronic Supplementary Information

### Reaction Mechanism between Small-Sized Ce Clusters and Water Molecules: An Ab Initio Investigation on $Ce_n+H_2O$

Table S1 The energies, compositions and occupancies of the high-energy molecular orbitals of the reaction products.

Isomers	Spin	Bond	Composition	Occupancy	Energy (a.u.)
CeO	$\alpha$	Ce(LP)	100%(6s <sup>0.91</sup> 6p <sup>0.04</sup> 4d <sup>0.05</sup> )	0.99	-0.13721
			100%(4f <sup>0.99</sup> )	1.00	-0.20270
		Ce-O	13%Ce(5d <sup>0.77</sup> 4f <sup>0.23</sup> )+87%O(2p <sup>1.0</sup> )	1.00	-0.30391
			13%Ce(5d <sup>0.77</sup> 4f <sup>0.23</sup> )+87%O(2p <sup>1.0</sup> )	1.00	-0.30391
			22%Ce(5d <sup>0.60</sup> 4f <sup>0.30</sup> )+78%O(2s <sup>0.13</sup> 2p <sup>0.87</sup> )	1.00	-0.49433
	$\beta$	Ce-O	11%Ce(5d <sup>0.76</sup> 4f <sup>0.23</sup> )+89%O(2p <sup>1.0</sup> )	1.00	-0.30463
			11%Ce(5d <sup>0.76</sup> 4f <sup>0.23</sup> )+89%O(2s <sup>0.04</sup> 2p <sup>0.96</sup> )	1.00	-0.30463
			21%Ce(5d <sup>0.68</sup> 4f <sup>0.24</sup> )+79%O(2s <sup>0.11</sup> 2p <sup>0.89</sup> )	1.00	-0.48379
	HCeOH	$\alpha$	Ce(LP)	100%Ce(6s <sup>0.69</sup> 5d <sup>0.25</sup> )	1.00
100%Ce(4f)				1.00	-0.23434
Ce-H			24%Ce(6s <sup>0.19</sup> 5d <sup>0.66</sup> 4f <sup>0.12</sup> )+76%H(1s <sup>1.0</sup> )	1.00	-0.26017
$\beta$		Ce-H	23%Ce(6s <sup>0.33</sup> 5d <sup>0.57</sup> 4f <sup>0.07</sup> )+77%H(1s <sup>1.0</sup> )	1.00	-0.25932
H <sub>2</sub> Ce <sub>2</sub> O	$\alpha$	Ce1(LP)	100%Ce1(6s <sup>0.69</sup> 5d <sup>0.21</sup> )	1.00	-0.11910
		Ce1(LP)	100%Ce1(4f)	1.00	-0.21410
		Ce2(LP)	100%Ce2(4f)	1.00	-0.21995
		CeH	18%Ce(6s <sup>0.20</sup> 5d <sup>0.66</sup> 4f <sup>0.10</sup> )+82%H(1s <sup>1.0</sup> )	0.86	-0.23772
		CeH	18%Ce(6s <sup>0.20</sup> 5d <sup>0.66</sup> 4f <sup>0.10</sup> )+82%H(1s <sup>1.0</sup> )	0.86	-0.23772
	$\beta$	Ce2(LP)	100%Ce2(4f)	0.95	-0.11222
		CeH	16%Ce(6s <sup>0.09</sup> 5d <sup>0.75</sup> 4f <sup>0.08</sup> )+84%H(1s <sup>1.0</sup> )	0.86	-0.23138
		CeH	16%Ce(6s <sup>0.09</sup> 5d <sup>0.75</sup> 4f <sup>0.08</sup> )+84%H(1s <sup>1.0</sup> )	0.86	-0.23138

HCe <sub>2</sub> OH	α	Ce1-Ce2	50%Ce1+50%Ce2(5d <sup>0.74</sup> 4f <sup>0.18</sup> )	1.00	-0.12588
		Ce1-Ce2	50%Ce1+50%Ce2(6s <sup>0.61</sup> 5d <sup>0.34</sup> )	1.00	-0.15049
		Ce2(LP <sup>2</sup> )	100%Ce2(4f)	1.00	-0.18618
		Ce1(LP <sup>1</sup> )	100%Ce1(4f)	1.00	-0.18620
		Ce-H	17%Ce(6s <sup>0.19</sup> 5d <sup>0.69</sup> )+83%H(1s <sup>1.0</sup> )	0.86	-0.22557
	β	Ce1-Ce2	50%Ce1+50%Ce2(6s <sup>0.28</sup> 5d <sup>0.66</sup> )	1.00	-0.11623
		Ce1-Ce2	50%Ce1+50%Ce2(6s <sup>0.41</sup> 5d <sup>0.52</sup> )	1.00	-0.15388
		Ce-H	16%Ce(6s <sup>0.16</sup> 5d <sup>0.71</sup> )+84%H(1s <sup>1.0</sup> )	0.87	-0.22809
H <sub>2</sub> Ce <sub>3</sub> O	α	Ce1-Ce3	43%Ce1(6s <sup>0.11</sup> 5d <sup>0.78</sup> )+57%Ce3(5d <sup>0.95</sup> )	0.73	-0.06841
		Ce2-Ce3	56%Ce2(6s <sup>0.55</sup> 5d <sup>0.40</sup> )+44%Ce3(6s <sup>0.32</sup> 5d <sup>0.62</sup> )	0.95	-0.13261
		Ce1-Ce3	55%Ce1(6s <sup>0.47</sup> 5d <sup>0.46</sup> )+45%Ce3(6s <sup>0.31</sup> 5d <sup>0.63</sup> )	0.96	-0.13822
		Ce1(LP)	100%Ce1(4f)	1.00	-0.17970
		Ce3(LP)	100%Ce3(4f)	1.00	-0.18680
	β	Ce2-Ce3	53%Ce2(6s <sup>0.46</sup> 5d <sup>0.48</sup> )+47%Ce3(6s <sup>0.24</sup> 5d <sup>0.73</sup> )	0.70	-0.05556
		Ce2-Ce3	33%Ce2(6s <sup>0.13</sup> 5d <sup>0.75</sup> )+67%Ce3(6s <sup>0.40</sup> 5d <sup>0.54</sup> )	0.76	-0.08027
		Ce2(LP)	100%Ce2(4f)	0.99	-0.17959
INT3	α	Ce2-Ce3	50%Ce2(6s <sup>0.23</sup> 5d <sup>0.70</sup> )+50%Ce3(5d <sup>0.85</sup> )	0.70	-0.08213
		Ce2-Ce3	43%Ce2(6s <sup>0.25</sup> 5d <sup>0.64</sup> )+54%Ce3(6s <sup>0.28</sup> 5d <sup>0.66</sup> )	0.76	-0.09457
		Ce1-Ce3	49%Ce1(6s <sup>0.54</sup> 5d <sup>0.39</sup> )+51%Ce3(6s <sup>0.49</sup> 5d <sup>0.48</sup> )	0.95	-0.16865
		Ce3(LP)	100%Ce3(4f)	0.99	-0.17951
		Ce1(LP)	100%Ce1(4f)	0.99	-0.19112
		Ce2(LP)	100%Ce2(4f)	1.00	-0.19693
	β	Ce2(LP)	100%Ce1(5d <sup>0.87</sup> )	0.35	-0.00253
		Ce1-Ce3	51%Ce1(5d <sup>0.93</sup> )+49%Ce3(5d <sup>0.92</sup> )	0.91	-0.10738
Ce2-Ce3		63%Ce2(6s <sup>0.49</sup> 5d <sup>0.44</sup> )+37%Ce3(6s <sup>0.24</sup> 5d <sup>0.70</sup> )	0.96	-0.15069	
Ce1-Ce3		69%Ce1(6s <sup>0.89</sup> )+31%Ce3(6s <sup>0.60</sup> 5d <sup>0.35</sup> )	0.97	-0.18440	